Capacitance based Tomography for Industrial Applications

Sharath Subash Donthi (04307905)
Supervisor: Prof. L. R. Subramanyan

Abstract- This paper discusses the applications of *Electrical Capacitance Tomography* systems in industries for studying the chemical processes taking place inside pipes and chemical vessels. It is a widely popular and non-intrusive technique for sensing and measuring the spatial distribution, voidage, and velocities of flow of the materials in a pipe. It helps the chemical process engineer in indirectly visualizing the chemical process taking place inside the vessel which until now was not possible. Capacitive sensors are employed to sense the change in permittivity of the materials inside the vessel. The acquired data is used to construct permittivity distribution images, which aid in understanding the nature of activities taking place inside the vessel, by calculating various key parameters related to the chemical process. The images can also help in deciding the future course of control actions needed to be taken if required. The advantages of the technique are non-intrusive nature for measuring the capacitances, simple transduction principle, fast response, simple and efficient algorithm used to generate images of reasonably good resolution. The sensors employed are capacitance sensors which are cost effective and easy to construct.

I. INTRODUCTION

The word 'tomography' is derived from the Greek words ‘tomos’ meaning ‘to slice’ and ‘graph’ meaning ‘image’. The Oxford English Dictionary defines Tomography as ‘Radiography in which an image of a predetermined plane in the body or other object is obtained by rotating the detector and the source of radiation in such a way that points outside the plane give a blurred image

The concept of Tomography was first published as early as 1826, by Abel, a Norwegian physicist, for an object with axis-symmetrical geometry. In 1917, an Austrian mathematician, Radon, extended Abel’s idea for objects with arbitrary shapes. Godfrey Hounsfield and Allen Cormack were jointly awarded the Nobel Prize in 1979 for their pioneering work on X-ray Tomography.

There exists a large demand for direct analysis of the internal characteristics of process plants in order to improve the design and operation of equipment. *Electrical Capacitance Tomography (ECT)* systems are gaining popularity day by day in the industrial sector. It is a technique for analyzing the process taking place insides pipes and chemical vessels by examining the internal distribution of permittivity. The study of the internal permittivity distribution requires a pictorial representation of the permittivity, which is possible by constructing permittivity distribution images. The images can be constructed by acquiring inter-electrode capacitances if the vessel is fitted with capacitive sensors. The measured inter-electrode capacitances aid in constructing the required permittivity distribution images by employing a suitable algorithm. The method of acquiring the data is non-intrusive, i.e., the flow inside the pipe is not disturbed, because the capacitance is measured outside the pipe. This hallmark has made the *ECT* systems superior to *Electrical Resistance Tomography (ERT)* systems which otherwise would have used intrusive techniques for measurements. Hence, the *ECT* systems have been reckoned for their various features, and are constantly replacing the previously used *ERT* systems for industrial tomography applications. However, this technique of non-intrusive measurement is still in the research sector [1].

The *ECT* system comprises of sensor, capacitance measuring unit, and control computer. The sensor is comprised of an array of electrodes wound around the periphery of the pipe or the vessel to be imaged. The measuring unit conditions the signal obtained from the sensor and transmits them to the control computer. The control computer processes the obtained information and constructs permittivity distribution images corresponding to cross-section viewed by the sensors. All the measured and calculated parameters are normalized to reduce the errors in measurement. The control computer employs the *Linear Back Projection Algorithm (LBPA)* for generating permittivity distribution images. The images are displayed on a 1024 square pixel grid using a suitable graduated color scale to indicate the variation of permittivity. The images are analyzed to compute the parameters related to the process like, spatial distribution and volume ratios of the materials inside the pipe, and the velocities of flow. *ECT* is being used in multi-phase flowmeters to

examine the flow regime of multiple fluids flowing in a pipe. The permittivity images are also used to generate appropriate control signals, which decide the future course of a chemical process.

II. MEASUREMENT SYSTEM CONFIGURATION

The ECT system shown in figure1 is used to obtain permittivity distribution images of contents of the pipe during a chemical process [2]. The system consists of the following:

1) C*apacitance sensor* which comprises of an array of electrodes attached to periphery of the pipe which is to be imaged.

2) C*apacitance measuring unit* to acquire and process the signals obtained from the capacitance sensor.

3) C*ontrol computer* to reconstruct and display the permittivity distribution image using the data obtained, and to monitor and control the process taking place inside the pipe.

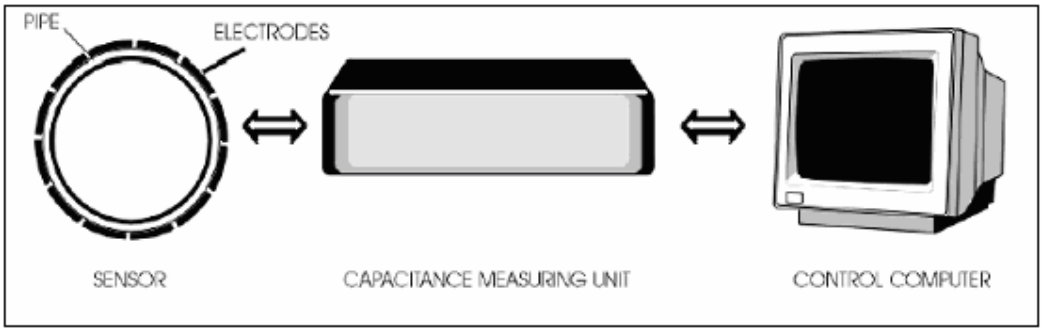

Figure 1-Electrical Capacitance Tomography System [2]

ECT System Description

Sensor

The sensor consists of an array of electrodes attached to the periphery of the pipe which is to be imaged. The pipe can be fitted with external electrodes or internal electrodes. Figure 2 shows their corresponding cross-sectional views.

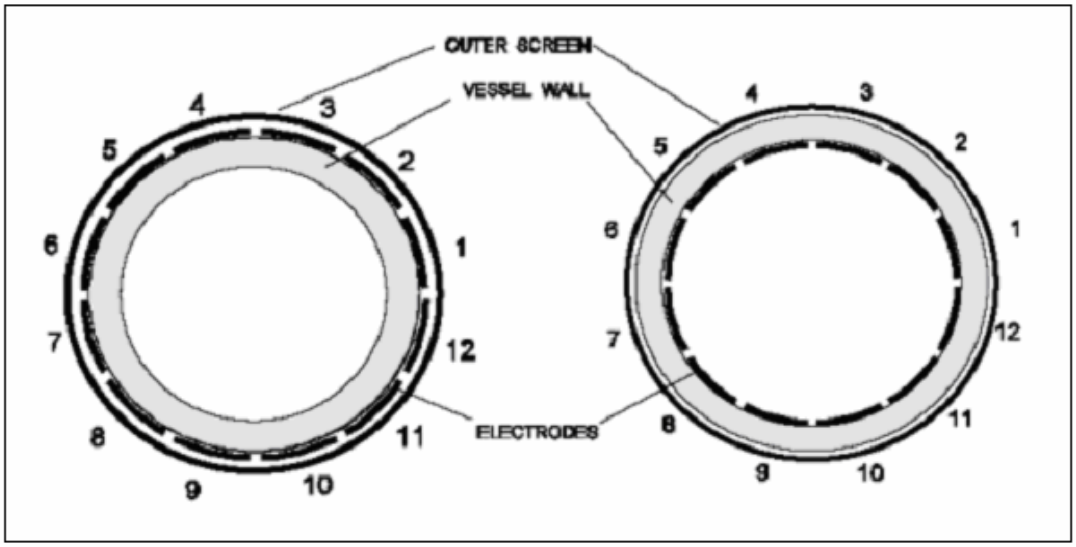

2 (a) External Electrodes 2 (b) Internal Electrodes

Figure 2-Cross-sections of sensors with external and internal electrodes [2]

Capacitance Measuring Unit

The capacitance measuring unit shown in figure 3 constitutes of the necessary electronic circuitry to measure and condition the signals received from the capacitance sensor. The various electronic circuits employed to accomplish these objectives are AC bridges for measuring capacitances, amplifiers, phase sensitive detectors, and filters.

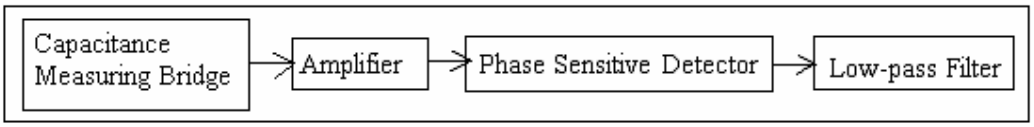

Figure 3-The building blocks of a capacitance measuring unit

The capacitance measuring bridge is an AC bridge which is used for measuring the inter-electrode capacitances of the sensor. The bridge comprises of four arms, of which one arm is used to accommodate the capacitance to be measured. The rest can be made of standard inductors, or capacitors or a combination of both capacitors and inductors. The most commonly used bridges are the transformer coupled ratio arm bridge and the Blumlein's bridge. When it comes to measuring very small capacitances the switched capacitor or the charge transfer technique is also used [3]. The signals received during measurements are generally weak and corrupted with noise. So, they need to be strengthened and purified to carry out further processing on them. Amplifiers are used to enhance the strength of the weak signals. The measured signals can have various extraneous signals riding over it. These are termed as noise signals. The noise signals corrupt the signal of interest and they need to be removed. *Phase Sensitive Detectors (PSD)* are used to detect signals of interest which lie hidden in a highly noisy signal. The output of the PSD comprises two components, namely, a DC signal and a high frequency signal. Filters are used to remove the noise present in them, and thereby, to recover the signal of interest. Typically we use an excitation signal of very small frequencies compared to the noise frequencies. Hence we need low-pass filters to filter out the high frequency noise signals from the output of the phase sensitive detectors.

Control Computer

There are a multitude of operations that need to be performed by the control computer. The signals acquired from the capacitance sensors are analog in nature. The control computer can process only digital signals. Hence the obtained signals have to be digitized. The unit which converts analog signals to digital signals is an *Analog to Digital Converter (ADC)*. The *ADC*s have sample and hold, and quantizer circuits which perform this task. The *ADC* can be a part of the measuring unit or the control computer. Most of the modern *ADC*s are available as plug and play cards which can be affixed onto a computer. Hence the digitization of analog signals is handled by the control computer itself.

The main role of the control computer is in constructing the permittivity distribution images using the data acquired by measuring the inter-electrode capacitances. For a 12-electrode *ECT* system, 66 independent inter-electrode capacitance measurements can be taken. The 66 measured capacitances have to be mapped onto a square grid containing 1024 pixels (32pixel X 32pixel) to graphically display the permittivity distribution inside the pipe. An algorithm implemented in the control computer performs the task of constructing the permittivity distribution images from the measured value of capacitances. In this process the control computer acts as a visual display unit.

The permittivity distribution images are used to interpret the process taking place inside the pipe. Every process is premeditated, and it is supposed to follow a desired course. When the process deviates from the desired path it needs to be externally controlled to bring it back to its original path. In this case, the control computer needs to generate the proper signals which control the process. These signals are generated after analyzing the permittivity distribution images.

III. CAPACITANCE SENSORS AND SENSOR FABRICATION

Sensors used for *ECT* systems are designed according to the cross-section of the vessel, and the positioning of the electrodes [4]. Most of current work is in the research sector where vessels with circular cross-sections are used. The electrodes can be mounted on the outside or on the inside of the vessel to be imaged. The choice of placing the electrodes depends on the material used to manufacture the pipe. If the pipe is made of conducting material, internal

electrodes are used. External electrodes are used if the pipe is made of insulating material. Both have their advantages and disadvantages.

Sensors with external electrodes are non-intrusive, and easy to design. They are not subjected to extreme temperatures, high pressures, and turbulences. Hence, they will not get contaminated by the fluid inside the pipe. The main drawback is the nonlinearity in its characteristics. The capacitance may increase or decrease with the change in permittivity inside the vessel depending on the thickness of wall of the vessel. Proper correction factors need to be applied in order to make the characteristics linear.

On the other hand, sensors with internal electrodes are complex to design as they have to withstand the extreme temperatures, high pressures, and turbulences. They need to withstand corrosion if the fluid inside is corrosive. But the change in capacitance is directly proportional to the change in permittivity inside the vessel. The linear characteristics exhibited by them prove to be their biggest advantage.

The *ECT* technique is very efficient for detecting permittivity changes inside a chemical vessel, when the vessel contains non-conducting or dielectric materials. The technique provides erroneous results when used to image a vessel containing conducting materials.

The magnitude of the inter-electrode capacitances is very small, of the order of fraction of a pico-Farad. The measurements can get corrupted due to extraneous earth capacitances which are larger in magnitude compared to the measured signals. To eliminate these stray effects, the electrodes are externally shielded irrespective of their placing. Another problem faced while measuring the capacitance is the fringing of electric filed between the electrodes. The fringing can be reduced to a great extent by using driven guard electrodes. The guard electrodes maintain parallel electric field lines and eliminate their axial spreading. They also improve the axial resolution and sensitivity of the sensor.

With the current state of capacitance measurement technology, it is possible to measure capacitance changes between 2 unearthed electrodes of 0.2 fF in the presence of stray capacitance to earth of 200pF at a rate of 2000 measurements per second. This sets a practical lower design limit on the capacitance between any pair of electrodes of around 10fF, which translates to measurement electrodes of minimum axial length 3.5cm for an 8 electrode sensor or 7 cm for a 12 electrode sensor. These dimensions assume that effective driven axial guards are used. For this condition to be met, the sum of the lengths of the axial guard and the measurement electrodes must equal or exceed the sensor diameter.

The choice of number of electrodes for measurement is a tradeoff between the axial and radial resolutions required, and the image acquisition rate. Typically, 12 electrodes are used to acquire images at a speed of 100 frames per second. The electrodes are placed and numbered as shown in figure 2. The number of electrodes is inversely proportional to both the image acquisition rate and the overall resolution.

For imaging a single vessel type with fixed cross-section and with a fixed electrode configuration, the measurement circuitry can be integrated into the sensor and the measurement circuits can be connected directly to the electrodes. This is the configuration for standardized industrial sensors. However, most current applications for *ECT* are in the research sector, where it is preferable to have a standard capacitance measuring unit which can be used with a wide range of sensors. Hence, the measuring unit and the sensor are segregated.

The typical values of inter-electrode capacitances for a sensor with 12 electrodes and above specified electrode lengths are indicated in figure 4. The units of capacitances are in femto-Farads.

The required electrode pattern can be designed using Computer Aided Design software and the electrodes fabricated using photolithographic techniques from a flexible copper-coated laminate. These are then wrapped around the outside of an insulating tube to form the sensor. Part of a design for an *E*-electrode single plane sensor with driven axial guards is shown in figure 5. *E* refers to the number of electrodes used. It shows earthed screening tracks between the sets of electrodes (to reduce the adjacent electrode capacitances) together with earthed areas at the ends of the sensor (to allow the cable screens to be terminated). Coaxial leads (with a maximum length of 2m to minimize capacitance to ground) are connected to the electrodes and an earthed screen is located around the sensor to exclude any external signals. Discharge resistors (typically 1 MO) must be connected between each electrode and the cable screen to ensure that no static charge can build up on the electrodes and connecting leads, otherwise

damage may occur when the sensor is connected to the capacitance measurement circuit. These basic techniques can be used to construct static or sliding sensors with internal or external electrodes. More complex fabrication techniques are needed for sensors for operation at elevated temperatures and pressures.

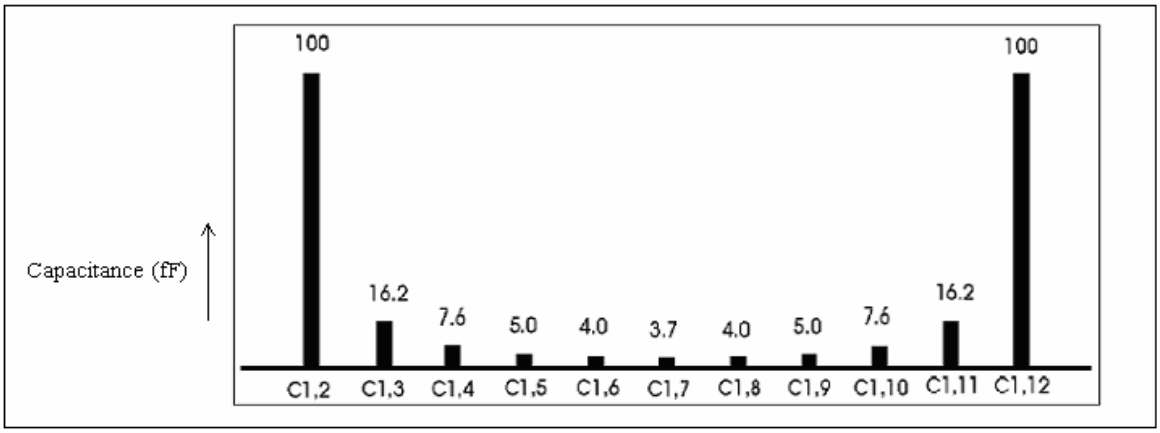

Figure 4-Typical values of inter-electrode capacitances for a 12-electrode ECT system [6]

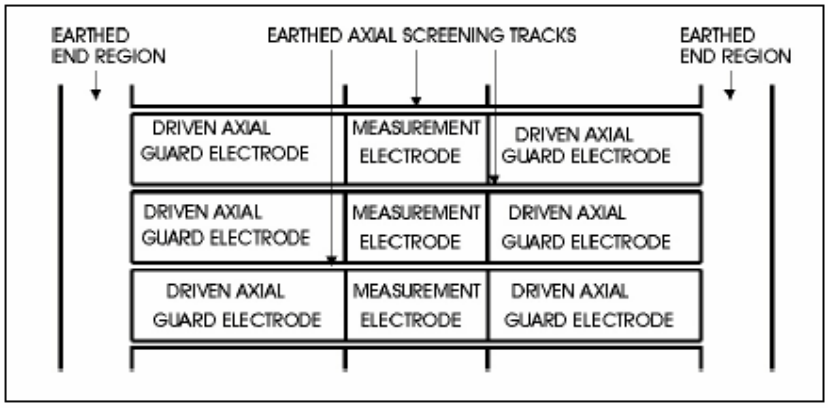

Figure 5-Partial PCB layout with N-electrode single plane sensor [2]

IV. MEASUREMENT PRESCRIPTS

Capacitance Measurement Protocols

Any measuring system has to follow certain protocols or sets of well-defined and properly established procedures to extract meaningful information from the sensor. Here the term protocol mainly refers to the sequence used to excite the sensor electrodes, and the order in which the signals are acquired.

In tomography, the object to be imaged is surrounded by electrodes, which act as both sources and detectors. The electrodes are excited one by one, or in pairs depending on the protocol used. At any point in time only one electrode or a pair of electrodes is excited, while the remaining electrodes function as detectors. Typically, *ECT* systems use 12 electrodes to acquire data regarding the inter-electrode capacitances. The data collected is used for constructing the permittivity distribution images in the subsequent stages. The electrodes are numbered as shown in figure 2 [5]. Different protocols can be devised as the capacitances between any two electrodes can be measured, and any sequence can be followed in exciting an electrode or a pair of electrodes.

Protocol 1 is the most widely used protocol in the industrial tomography systems. Here, only one electrode is excited at any point in time and the remaining electrodes function as detectors. The capacitance between the source electrode and the remaining detector electrodes are measured for all the possible pairs. Subsequently, the next electrode is made the source and the same measurement process is employed. For example, if electrode 1 is made

the source electrode, rest 11 electrodes function as detector electrodes. The detector electrodes are connected to the virtual ground terminals, so that they remain at zero potential with respect to ground. The capacitances between electrode 1 and the others are measured. After measuring all the possible pairs of capacitances, electrode 2 is made the source electrode and the measurement process is repeated. The whole cycle of exciting an electrode and measuring the resulting inter-electrode capacitances is repeated.

In higher order protocols like protocol 2 and protocol 3 electrodes are excited in pairs and the inter-electrode capacitances are measured for various combinations of the detector electrodes. This increases the number of possible measurements, and improves the resolution of images too. However, this reduces the image acquisition rate.

For an *ECT* system having *E* electrodes and using protocol number *P*, the number of independent inter-electrode capacitance measurements *M* is given in (1).

$$M = \frac{E(E-(2P-1))}{2} \tag{1}$$

Protocol 1 is highly compatible with *LBPA* for reconstructing of the permittivity distribution images using the measured inter-electrode capacitances. *LBPA* is moderately efficient and fast when it comes to on-line reconstructing of images. It is the most preferred algorithm for reconstructing permittivity distribution images in the industry. For a typical capacitance sensor with 12 electrodes and using protocol 1, 66 independent inter-electrode capacitances can be measured.

V. PERMITTIVITY AND CONCENTRATION MODELS

ECT systems are used to create permittivity distribution of the contents of the pipe by measuring the inter-electrode capacitances. *ECT* systems work well for a two-component system, which is modeled as a combination of two substances having different relative permittivities [6]. By default, air is assumed to be one of the components. Air has a relative permittivity of *1*. Let the other component have a dielectric constant *k*. The capacitance between any two electrodes is given in (2).

$$C = \frac{A\varepsilon_0 k}{d} \tag{2}$$

Where *A* is the area of cross-section of the electrodes, ε_0 is the permittivity of free space, and *d* is the distance between the electrodes. The dielectric constant *k* is same as the relative permittivity ε_r.

The capacitance measured depends on the relative permittivity of the materials between the electrodes. Their relation can be linear or nonlinear in nature. It depends on the permittivity models used to characterize the way in which the contents occur. The various permittivity models used are the series model, parallel model, and Maxwell's model.

Suppose two substances are mixed together and one of the substances is air. Let the other substance have a relative permittivity ε_r and occupy *x*% of the total space between two electrodes. The effective permittivity of the mixture and their dependence on capacitance for various models are explained in the following sections.

Series Permittivity Model

If the two components in the pipe occur as discrete bands and lie on top of one another, the effective capacitance can be considered as two capacitances connected in series. This is illustrated in figure 6. In this case, the capacitance and permittivity are related in a nonlinear fashion. The effective permittivity and overall capacitance is given in (3) and (4) respectively.

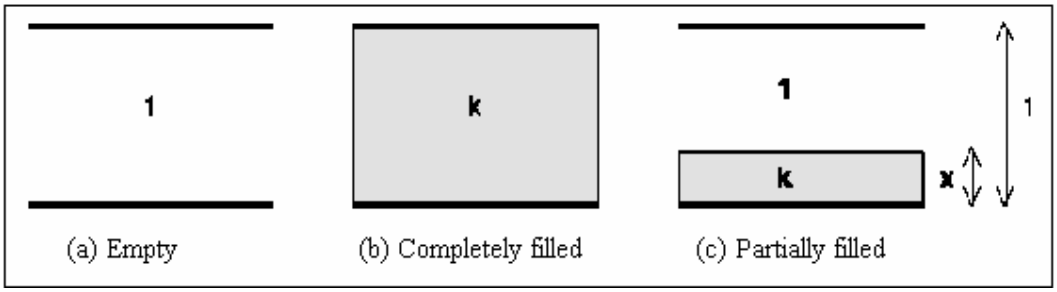

Figure 6-The series permittivity model [6]

$$\varepsilon_s = \frac{\varepsilon_0 \varepsilon_r x(1-x)}{1-x(\varepsilon_r - 1)} \tag{3}$$

$$C_s = \frac{A\varepsilon_s}{d} \tag{4}$$

Parallel Permittivity Model

If the two components in the pipe occur as discrete bands and appear alternatively, their effective capacitance can be considered as two capacitances connected in parallel. This is illustrated in figure 7. In this case, the capacitance and permittivity are related linearly. The effective permittivity and overall capacitance is given in (5) and (6) respectively.

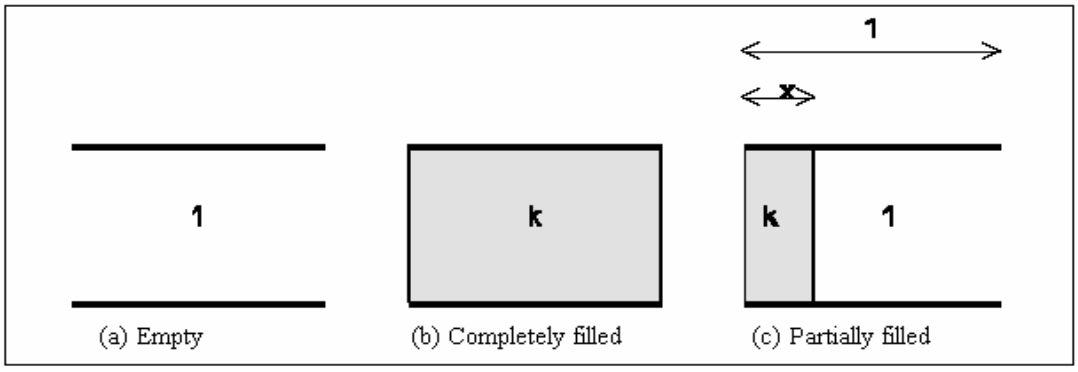

Figure 7-The parallel permittivity model [6]

$$\varepsilon_p = \varepsilon_0[1 + x(\varepsilon_r - 1)] \tag{5}$$

$$Cp = \frac{A\varepsilon_p}{d} \tag{6}$$

Maxwell's Permittivity Model

This modeling is used when the nature of distribution of the materials in the pipe is random. If two materials of relative permittivities ε_1 and ε_2 are mixed, then the effective permittivity and overall capacitance of the combination is given in (7) and (9) respectively.

$$\varepsilon_m = \frac{\varepsilon_1[2\varepsilon_1 + \varepsilon_2 - 2x(\varepsilon_1 - \varepsilon_2)]}{2\varepsilon_1 + \varepsilon_2 + x(\varepsilon_1 - \varepsilon_2)} \tag{7}$$

Since air is one of the contents, $\varepsilon_1 = 1$. Hence, (7) can be simplified to (8)

$$\varepsilon_m = \frac{[2+\varepsilon_2 - 2x(1-\varepsilon_2)]}{2+\varepsilon_2 + x(1-\varepsilon_2)} \tag{8}$$

$$C_r = \frac{A\varepsilon_m}{d} \tag{9}$$

VI. NORMALIZATION OF MEASURED CAPACITANCES AND PERMITTIVITIES

All the measured inter-electrode capacitances and the subsequently obtained permittivities are normalized before constructing the permittivity distribution images [6]. The absolute value of measured inter-electrode capacitances C_{MA}, is normalized to C_N according to (10). C_{MA} is calculated from (12)

$$C_N = \frac{C_{MA} - C_{LA}}{C_{HA} - C_{LA}} \tag{10}$$

C_{HA} = the absolute value of the capacitance measured during calibration, when the sensor is completely filled with higher permittivity material. This is obtained from (13)

C_{LA} = the absolute value of the capacitance measured during calibration, when the sensor is completely filled with lower permittivity material. This is obtained from (14)

In a similar fashion the permittivities K_{MA} obtained from (4), (6), and (9) by measuring the inter-electrode capacitances are normalized to K_N using (11).

$$K_N = \frac{K_{MA} - K_{LA}}{K_{HA} - K_{LA}} \tag{11}$$

K_{HA} = the absolute value of the permittivity obtained during calibration, when the sensor is completely filled with higher permittivity material.

K_{LA} = the absolute value of the permittivity obtained during calibration, when the sensor is completely filled with lower permittivity material.

The normalized values of capacitances and permittivities lie between *0* and *1*. The normalized value will be *0* when the sensor is completely filled with the lower permittivity material. The value will be *1* when the sensor is completely filled with the higher permittivity material. These values set the lower and upper limit of the normalized capacitance curve and normalized permittivity curve.

The pixel values in the permittivity image are similarly normalized, so that they have the value *0* for the lower permittivity material, and *1* when the sensor is filled with the higher permittivity material.

There are many advantages of dealing with normalized values of quantities. They are as follows:

1) It eliminates the need to know the characteristic constants of the individual materials inside the sensor.
2) The widely different ranges of capacitance measurements, permittivity values, and pixel values are reduced to a single measurement range from *0* to *1*.
3) The effect of measurement errors inside the unit like offset and drift are eliminated.
4) The calibration of the sensor becomes easy.

While measuring the capacitance between a pair of electrodes, the first measurement is taken by connecting one electrode to excitation and the other one to measuring circuit. This capacitance is denoted by C_M. A second measurement of capacitance between the same pair of electrodes is taken, but this time setting the excitation to zero. In principle, the measured capacitance under these conditions should be zero. However, in practice a finite

(but normally small) capacitance is measured with the excitation voltage set to zero. This capacitance is caused by spurious capacitive coupling of the CMOS switch gate control waveforms into the capacitance measurement circuit and is known as the charge injection capacitance C_0.

Hence, the actual measured capacitance is given in (12).

$$C_{MA} = C_M - C_0 \tag{12}$$

In a similar fashion C_{HA} and C_{LA} can be calculated from the measured values of C_H and C_L using (13) and (14).

$$C_{HA} = C_H - C_0 \tag{13}$$
$$C_{LA} = C_L - C_0 \tag{14}$$

The absolute values of capacitances obtained from (12), (13), and (14) are substituted in (10) to obtain the normalized capacitances during measurement. This value is not corrupted by any errors introduced by the system.

The normalized capacitance and permittivity graphs are shown in figure 8(a) and 8(b) respectively.

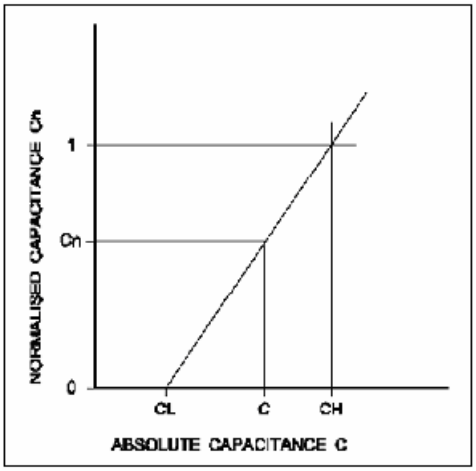

8(a)

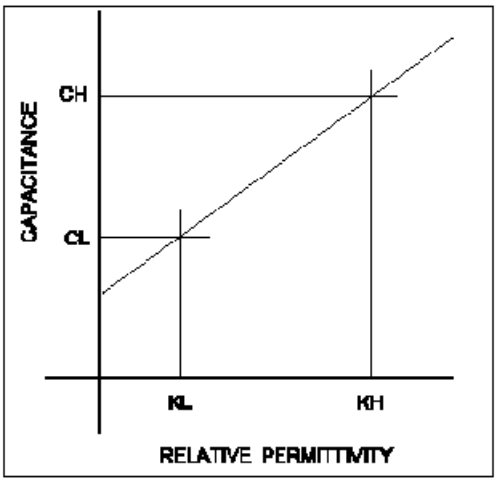

8(b)

Figure 8- (a) Normalized capacitance graph, and (b) Normalized permittivity graph [6]

The normalized permittivity values are then mapped onto a (32 X 32) square pixel grid where the pixel values are similarly normalized to lie between 0 and 1. This greatly simplifies the mapping. A pixel whose value is 0 is indicated in blue and a pixel having value 1 is indicated in red. The intermediate values are correspondingly represented by colors that lie between blue and red varying gradually.

VII. CONSTRUCTION OF PERMITTIVITY DISTRIBUTION IMAGES

Permittivity distribution images are the means of studying a chemical process where two materials having different relative permittivities react inside a vessel. This is achieved by positioning capacitance sensors around the periphery of the vessel. The capacitances are monitored continuously according to protocol 1. The measured inter-electrode capacitances, 66 in number for a 12-electrode ECT system, need to be projected onto a (32 X 32) square pixel grid to generate the current permittivity distribution image. One set of inter-electrode measurements is required to reconstruct one permittivity distribution image [5].

Figure 9 shows a (32 X 32) square pixel grid used to display the permittivity distribution image of an 8-electrode sensor having circular cross-section. To create an image only those pixels are used which lie inside the cross-sectional view of the vessel. The remaining ones are unused. Hence, on a (32 X 32) square pixel grid containing 1024 pixels, only 812 pixels are needed to construct the cross-sectional image of the vessel. The remaining pixels which lie outside the cross-sectional view of the vessel are not required and hence neglected.

Since the sensor has a circular cross-section and the electrodes are affixed to the circumference of the vessel, the electric filed lines that exist between any two electrodes are not straight. The field lines are curved instead. But they can be approximated to suit the requirement. Hence, proper sensitivity maps have to be developed for visualizing the electric field established between two electrodes when one of them is excited. The sensitivity maps aid in selecting the proper pixel that individually contributes to the capacitance changes (this information is used during calibration) and the intensities a pixel is subjected to.

Figure (10) shows the sensitivity maps for an 8-electrode circular sensor when the whole sensor is filled with higher permittivity material. In this case all the normalized values of capacitances between the electrodes, permittivity, and pixel values will have a value 1. Therefore the pixels which contribute to the electric lines of force are indicated in red. In figure 10, electrode 1 is made the source electrode and the approximated electric field lines that exist between electrodes 1and 2, electrodes 1 and 3, electrodes 1and 4, and electrodes 1and 5 are illustrated. The electric field lines that exist between electrode 1 the other electrodes 6, 7, and 8 will be the mirror images of the field lines that exist between electrode 1 and electrodes 4, 3, and 2 respectively. This approximation of the distribution of field lines works well when the

LBPA is used to reconstruct the permittivity distribution images. Research has proved that this approximation and the methodology used, suffices the industry requirement to study the mixture of two fluids by analyzing the reconstructed permittivity distribution image.

The permittivity distribution of a mixture of two fluids is often displayed as a series of normalized pixels located on a (32 X 32) square pixel grid, using an appropriate color scale to indicate the normalized pixel permittivity (as shown, for example, in figure 11). This uses a graduated blue/green/red color scale, where pixel values corresponding to the lower permittivity material used for calibration have the value zero and are shown in blue, while pixels corresponding to the higher permittivity material have the value 1 and are shown in red. The normalized permittivity distribution corresponds to the fractional concentration distribution of the higher permittivity material.

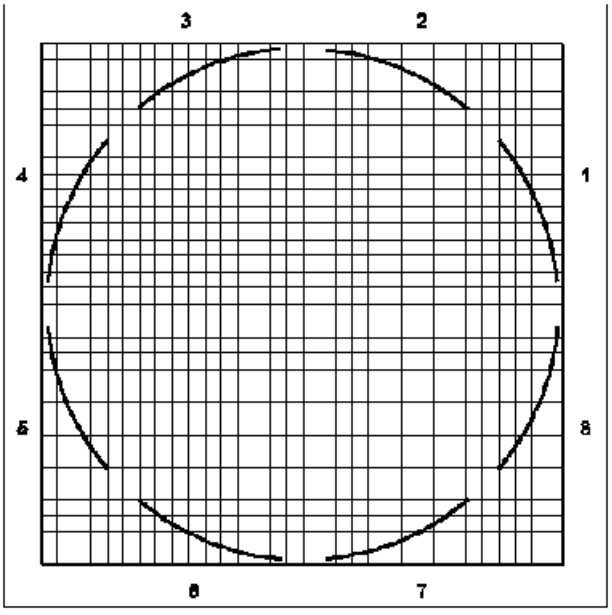

Figure 9-A 1024 pixel grid (32 X 32 pixel) used to image the contents of a vessel fitted with 8 electrodes [5]

Sensor Calibration and the Sensitivity Matrix

The real challenge in using ECT systems for creating permittivity distribution lies in constructing images on a 1024 square pixel grid using limited number of inter-electrode capacitance measurements. For a 12-electrode *ECT* system a maximum of 66 independent inter-electrode capacitance measurements are possible. These 66 measurements have to be projected onto 812 pixels on a 1024 square pixel grid. It is mathematically impossible to carry out this calculation accurately as there is insufficient information available due to the limited number of

electrode-pair capacitance measurements. The task therefore reduces to finding the best possible approximate solution to the problem. It has to be tackled by developing effective calibration and reconstruction techniques.

The calibration handles the forward problem of obtaining the required values of inter-electrode capacitances to create a particular deducible pattern on the image grid. The *LBPA* technique is used to solve the reverse problem of obtaining the individual values of 812 pixels from the acquired capacitance measurements. A suitable transform has to be developed to cater these requirements.

The forward and reverse problem solutions are arrived at considering a 12-electrode capacitance sensor which yields 66 independent inter-electrode capacitance measurements for a single frame of image.

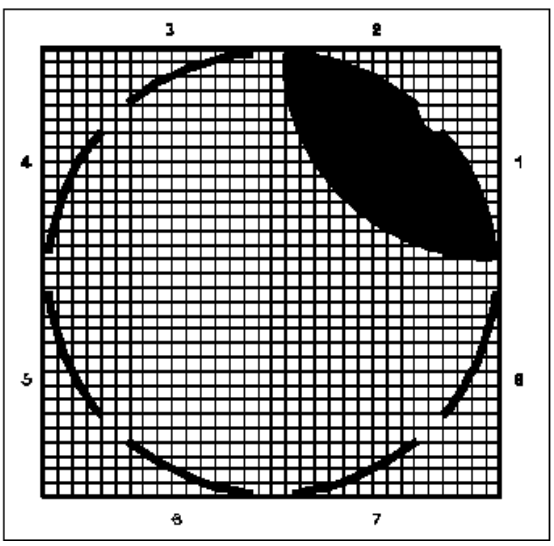

10 (a)

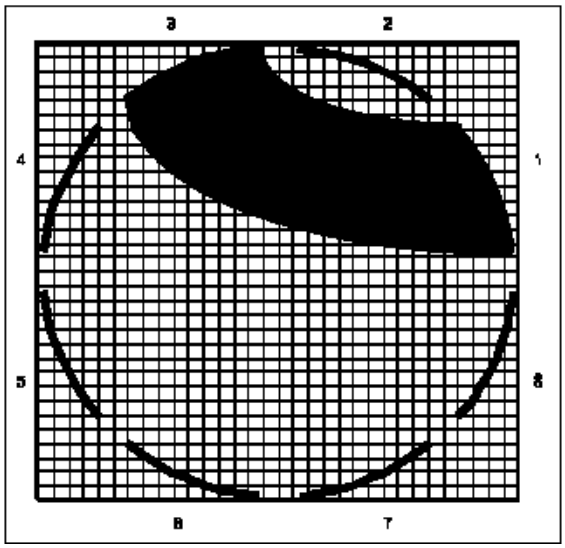

10 (b)

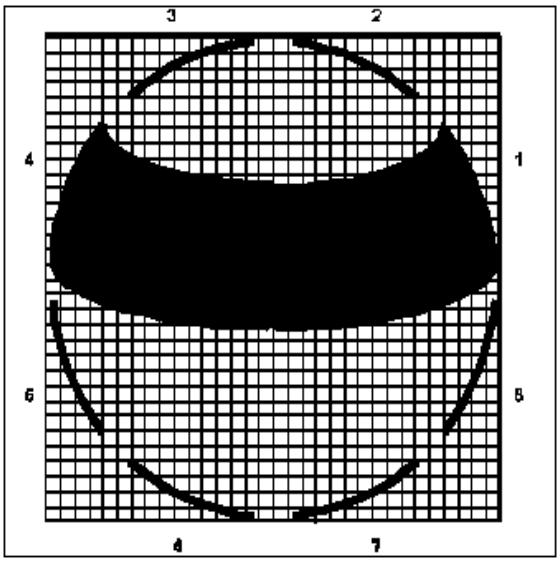

10 (d)

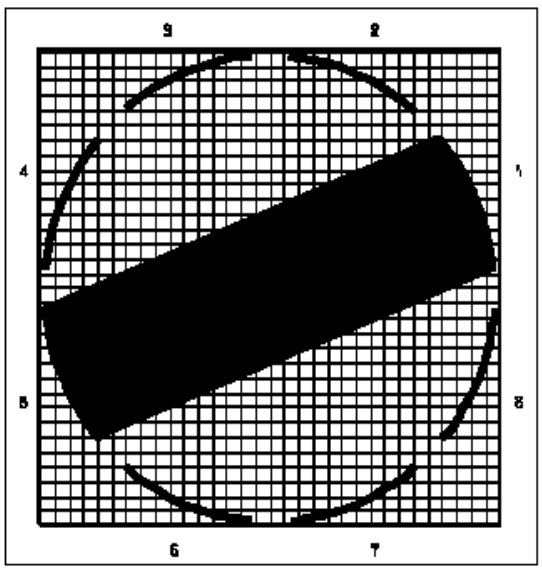

10 (d)

Figure 10-The electric filed lines established between (a) electrodes 1and 2, (b) electrodes 1 and 3, (c) electrodes 1 and 4, and (d) electrodes 1 and 5, with electrode 1 being the source electrode [5]

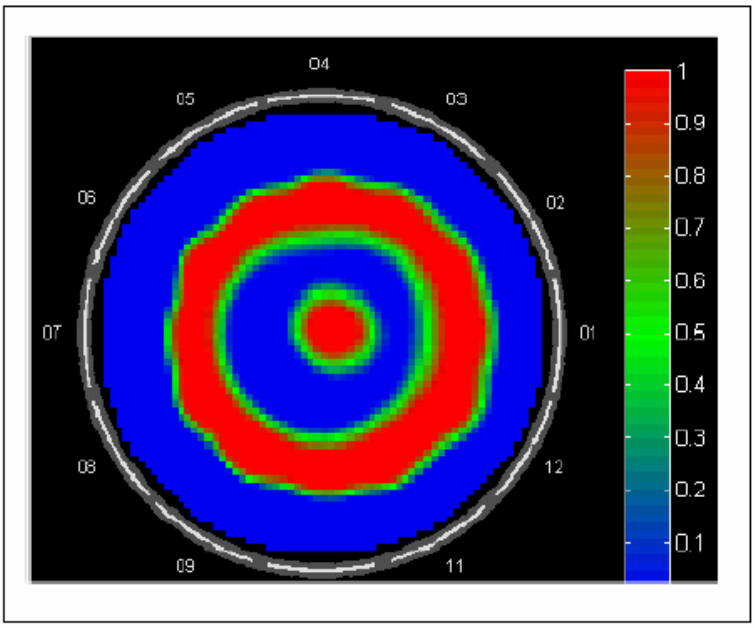

Figure 11-Using normalized pixel permittivity values to display a typical permittivity distribution image [2]

Forward Problem

The forward problem deals with the generation of 66 capacitance values required to produce a particular permittivity distribution image.

The forward transform is given in (15).

$$[C] = [S][K] \tag{15}$$

[C] = M X 1 matrix containing the normalized electrode-pair capacitances C_m (in the nominal range 0 to 1). M will have a value of 66 for a 12-electrode sensor. The number of elements in [C] indicates the total number of possible inter-electrode capacitance measurements using a certain protocol. This value can be obtained from (1).

[K] = N X 1 matrix containing the normalized pixel permittivities (in the nominal range 0 to 1) $\boldsymbol{N}$ is the number of pixels representing the sensor cross-section. $\boldsymbol{N}$ will be 812 for a 32 x 32 square pixel grid. The number of elements in [N] indicates the total number of pixels required to image a vessel having a particular cross-section on a 1024 square pixel grid. This value can be deduced from figure 9 by counting the number of pixels required to accommodate the vessel periphery on a 1024 square pixel grid.

[S] = M X N matrix containing the set of sensitivity matrices for each electrode-pair. The matrix S is commonly referred to as the *sensitivity map* or the *sensor sensitivity matrix* of the sensor.

One method for calculating the sensitivity coefficient S of a pixel for an electrode-pair (i-j) is based on the use of equation (16).

$$S = \int_A E_i . E_j dA \tag{16}$$

where E_i is the electric field inside the sensor when one electrode of the pair i is excited as a source electrode, E_j is the electric field when electrode 'j' is excited as a source electrode and the dot product of the two electric field vectors E_i and E_j is integrated over the area 'A' of the pixel. The set of sensitivity coefficients for each electrode-pair is known as the sensitivity map for that pair. For circular sensors with either internal or external electrodes, it is possible to derive an analytical expression for the electric fields and in this case, the sensitivity coefficients (and also the electrode capacitances) can be calculated accurately. For more complex geometries, numerical methods can be used to calculate the sensitivity coefficients. It is normally only necessary to calculate a few primary sensitivity

maps for the unique geometrical electrode pairings, as all of the other maps can be derived from these by reflection or rotation.

A typical forward transform matrix for a 12-electrode sensor, projecting the measurements onto 812 pixels on a 1024 square pixel grid is given in (17).

$$\begin{bmatrix} C_1 \\ C_2 \\ - \\ - \\ C_{66} \end{bmatrix} = \begin{bmatrix} S_{1,1} & S_{1,2} & - & - & S_{1,812} \\ S_{2,1} & S_{2,2} & - & - & S_{2,812} \\ - & - & - & - & - \\ - & - & - & - & - \\ S_{66,1} & S_{66,2} & - & - & S_{66,812} \end{bmatrix} \begin{bmatrix} K_1 \\ K_2 \\ - \\ - \\ K_{812} \end{bmatrix} \tag{17}$$

The forward problem addresses the need to calculate the value of inter-electrode capacitances required to produce a permittivity distribution image under two conditions. In the first case, the sensor is completely filled with the higher permittivity material and the required normalized capacitances or the elements of matrix *[C]* are calculated. Here the individual values of matrix *[K]* will be 1 because we have considered vessel is completely filled with the higher permittivity material. Hence all the pixels are active and correspond to the highest normalized vale 1. The elements of *[S]* are calculated from the sensitivity maps indicated in figure 10. Each element corresponds to a certain number *D* for a particular capacitance between a pair of electrodes. The number *D* indicates the contribution by the pixel towards indicating the amount of higher permittivity material present in that particular pixel. The values of *D* lie between 0 and 1. Suppose a particular pixel is partly covered, say 76%, the value of that element in the matrix *[S]* will be0.76. The presence of higher permittivity material is indicated in red.

In the second case the tank is completely filled with the lower permittivity material. Air is regarded as the lower permittivity material in almost all the cases. Here the normalized values of the inter-electrode capacitances, permittivity, and the pixel values will be 0. The presence of the lower permittivity material is indicated in blue.

Reverse Problem

The reverse problem addresses the issue of creating the permittivity distribution images from the obtained values of inter-electrode capacitances. To accomplish this, the value of the individual pixels are needed, i.e., the individual contribution of each pixel to the permittivity distribution image. The individual contribution is nothing but their normalized values. Since the 66 inter-electrode capacitances can be acquired on a continuous basis, need arises to calculate the normalized values of 812 pixels. The relation can be found in (18) which in turn is obtained from (15).

$$[K] = [Q][C] \tag{18}$$

Where $[Q] = [S]^{-1}$, is the inverse of the sensor sensitivity matrix *[S]* obtained during the formulation of the forward problem.

But mathematically it is not easy to find the inverse of a non-square matrix. Hence, the relation given in (18) cannot be used though it looks possible. Hence, the reverse problem is solved using the *LBPA*. As an exact inverse matrix does not exist, an approximate matrix must be used. The *LBPA* uses the transpose of the sensitivity matrix, $[S]^T$ which has the dimensions *(N X M)* and this is justified by the following reasoning: Although there exists no means of knowing which pixels have contributed to the capacitance measured between any specific electrode-pair, we know from the sensitivity matrix *[S]* that certain pixels have more effect than others on this capacitance. Consequently, component values are allocated to each pixel which will be proportional to the product of the electrode-pair capacitance and the pixel sensitivity coefficient for this electrode-pair. This process is repeated for each electrode-pair capacitance in turn and the component values obtained for each pixel are summed for the complete range of electrode-pairs. This simple algorithm produces approximate, but very blurred permittivity images, and a typical image, for a dielectric tube inside a 12-electrode sensor, is shown in figure 12. The *LBPA* acts as a spatial filter with a lower cut-off frequency than that of the fundamental filter (as shown in figure 13) and produces sub-optimal images from a given set of input data.

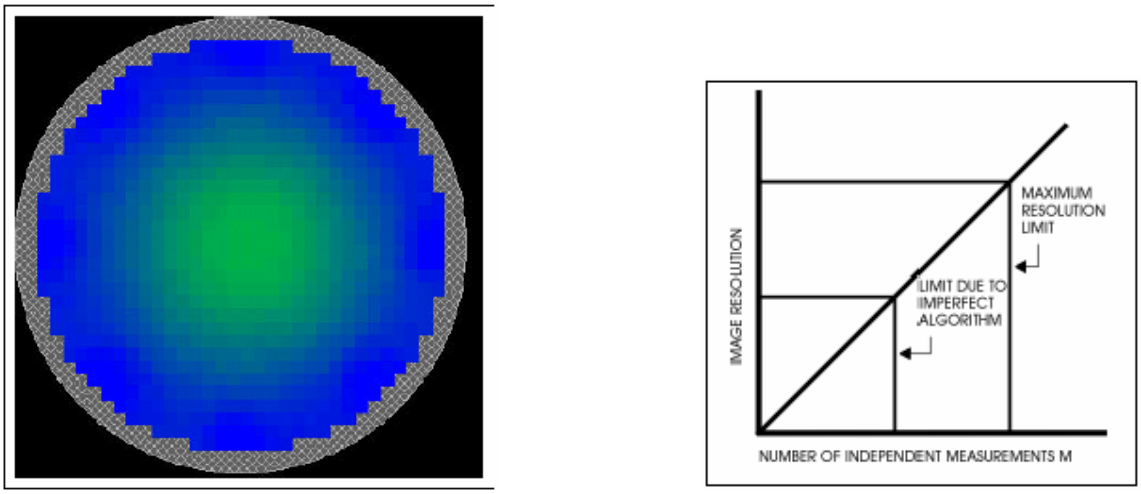

(a) (b)

Figure 12- (a) The image obtained using *Linear Back Projection* technique for a dielectric tube inside a 12-electrode sensor, (b) the spatial filter resolution limits [7]

The matrix used to calculate the normalized pixel values is given in (19).

$$\begin{bmatrix} K_1 \\ K_2 \\ - \\ - \\ K_{812} \end{bmatrix} = \begin{bmatrix} S_{1,1} & S_{2,1} & - & - & S_{66,1} \\ S_{1,2} & S_{2,2} & - & - & S_{66,2} \\ - & - & - & - & - \\ - & - & - & - & - \\ S_{1,812} & S_{2,812} & - & - & S_{66,812} \end{bmatrix} \begin{bmatrix} C_1 \\ C_2 \\ - \\ - \\ C_{812} \end{bmatrix} \tag{19}$$

VIII. ITERATIVE METHODS FOR IMPROVING IMAGE QUALITY

The images constructed using *LBPA* techniques are very blurred and have very poor resolution, and the resolution obtained way less than the actual image resolution. The inherent disadvantages of *LBPA* technique are

1) The pixels which have normalized value of 1 have been assigned a value below 1. In general, the *LBPA* will always under-estimate areas of high permittivity.

2) Some of the pixels which should have zero values have had finite values assigned to them. In general, the *LBPA* will over-estimate areas of low permittivity.

3) The sum of the calculated pixel permittivities equals that of the original single probe pixel. In general, the average permittivity of all of the pixels calculated by the *LBPA* will approximately equal that of the sensor when it contains the test object. The *LBPA* is therefore useful for calculating the volume ratios of contents of the sensor.

However, the main advantage of *LBPA* technique lies in its speed of capturing the images, but for a good image the resolution needs to be increased further. This can be done by implementing iterative methods. Iterative methods calculate the errors introduced in normalized values [7]. These errors are included in subsequent normalized value calculations to calculate the next set of normalized values. Again the errors are found out and the cycle is repeated until the error value becomes zero. In short, the function of iterative techniques is analogous to the technique used to achieve stability in a negative feedback control system. The iterative technique reduces the errors and, consequently the images obtained are of superior quality compared to the ones constructed using *LBPA* technique. Figure 13 shows some of the images for a certain number of iterations performed on figure 12 (imaging a dielectric tube in a 12-electrode sensor) obtained using *LBPA* technique.

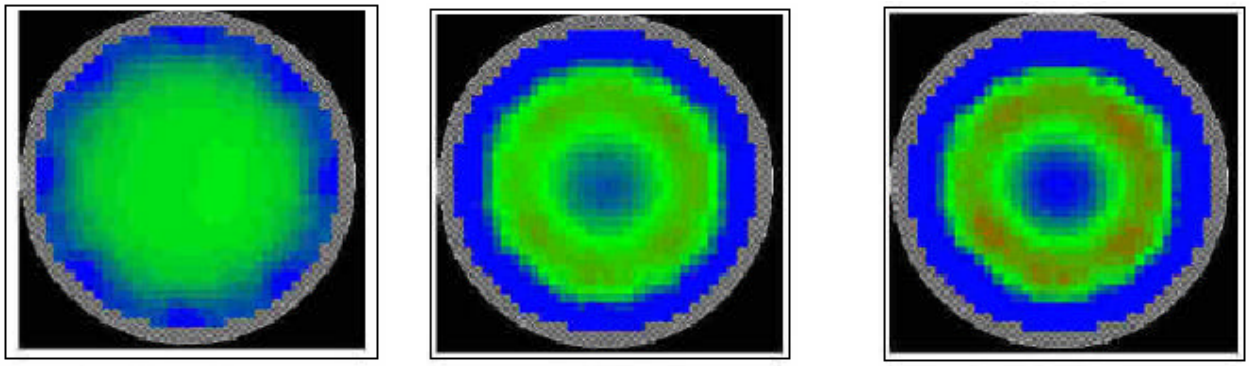

(a) (b) (c)

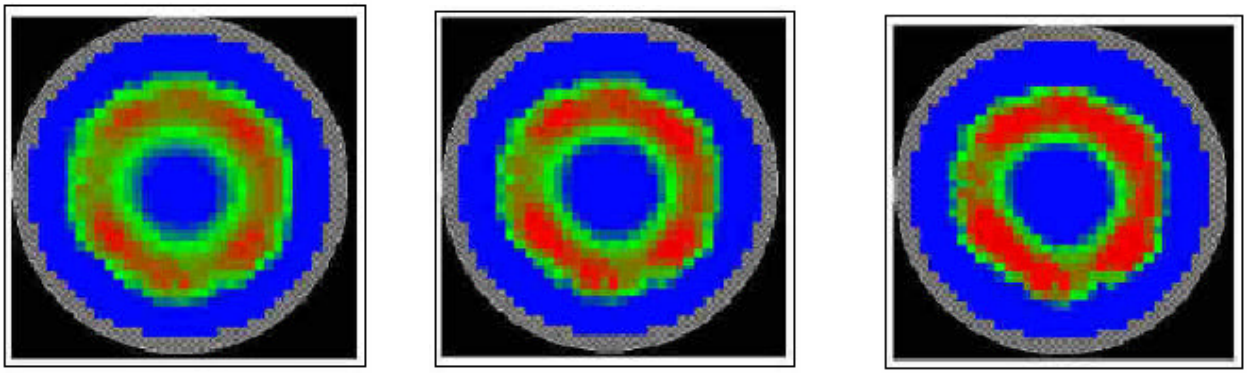

(d) (e) (f)

Figure 13-(a) by Linear Back Projection Algorithm, (b) after 10 iterations, (c) after 20 iterations, (d) after 50 iterations, (e) after 100 iterations, (f) after 200 iterations [7]

The main advantage of using iterative technique is the improved image resolution. The number of iterations used is decides the image capture rate and the relation is directly proportional. Hence, more number of iterations is used only when high resolution images are required. But with the availability of high speed computing and modern electronics it is possible to use *LBPA* techniques equipped with high number of iterative procedures and still capture image at a sufficiently high rate.

IX. APPLICATIONS OF ECT IMAGES

Measurement of Volume Ratio [8]

It is desirable to calculate the overall voidage or volume ratio of the materials present in the vessel at any point in time. The volume ratio gives information about the spatial distribution of a mixture of two different dielectric materials (a two-phase mixture). From this permittivity distribution, it is possible to obtain the distribution of the relative concentration (volume ratio) of the two components over the cross-section of the vessel. Voidage or volume ratio is defined as the percentage of the volume of the sensor occupied by the higher permittivity material. This figure can be calculated in two ways, either by using the normalized capacitance values obtained from the inter-electrode capacitance measurements, or from the normalized permittivity distribution values obtained from the permittivity distribution images. The optimum choice depends on the permittivity model used to model the presence of materials inside the vessel. For some applications**,** such as liquid or dense-phase mixtures, the parallel permittivity model can be used to obtain the voidage distribution directly from the permittivity distribution of the mixture. However, in other applications, such as fluidized beds with high levels of fluidization, the series permittivity model produces better accuracy and sensitivity. Maxwell's model which combines both parallel and series models is a useful compromise in many practical applications.

A typical *ECT* permittivity image format uses a square grid of 32 x 32 pixels to display the distribution of the normalized composite permittivity of each pixel. For a circular sensor, 812 pixels are used to approximate the

cross-section of the sensor. The values of each pixel represent the normalized value of the effective permittivity of that pixel. In the case of a mixture of two dielectric materials, these permittivity values are related to the fraction of the higher permittivity material present, i.e., the volume ratio at that pixel location. Using these values, the overall volume ratio can be calculated. The volume of the sensor is the product of area of cross-section of the sensor and the axial length of the sensor measurement electrodes.

All voidage values obtained from the *ECT* system are based on the assumption that the voidage is 100% when the sensor is full of the higher permittivity material and is zero when the sensor is filled with the lower permittivity material. Consequently, the voidage values obtained from an ECT system are relative voidages.

The absolute voidage of the pixel *VR* is given in (20).

$$VR = p.f \tag{20}$$

Where p is the relative voidage value of the pixel, and f is the absolute voidage when the sensor is filled with higher permittivity material.

If the absolute voidage is calculated from the permittivity distribution images, then it is done so by summing the normalized pixel values of all the pixels averaged over the total number of pixels. This relation is given in (21).

$$VR = \frac{1}{N}\sum_{i=1}^{N}\frac{P_i}{P_k} \tag{21}$$

Where, N is the total number of pixels, P_i is the normalized value of the i^{th} pixel, and P_k is the normalized value of the i^{th} pixel when the sensor is completely filled with higher permittivity material (nominally 1).

If the average voidage is calculated from the inter-electrode capacitance measurements, then it is done so by summing all the normalized capacitance values required to produce one frame of image, averaged over the total number of measurements per image frame. The relation is given in (22).

$$VR = \frac{1}{M}\sum_{j=1}^{M}\frac{C_j}{C_k} \tag{22}$$

Where, M is the total number of inter-electrode capacitances measured, C_j is the normalized value of the individual inter-electrode capacitance of the j^{th} pair, and C_k is the normalized value of the inter-electrode capacitance of j^{th} pair when the sensor is completely filled with the higher permittivity material (nominally 1).

In the parallel permittivity model, the capacitance is directly proportional to the relative permittivity. Hence the normalized pixel permittivity is directly proportional to the volume of the higher permittivity material present. Therefore, the volume ratio can be arrived at by using either (21) or (22) because of the linear relation.

In series permittivity model and Maxwell's model the relation between the normalized pixel values and the relative permittivity is non-linear and hence the volume ratio cannot be calculated by (21) before applying the proper correction factors. (22) is used to calculate the volume ratio in these cases.

Measurement of Flow [2]

In principle, *ECT* can be used to measure the flow of a fluid mixture by measuring the concentration profiles K at two measurement planes simultaneously and by using correlation techniques to extract the velocity profile V. The flow profile is the product $K.V$ and the flow rate is obtained by integrating the flow profile over the cross sectional area. In practice, the frame rates achievable with *ECT* at present limit the use of this technique to situations where the fluid mixture is moving relatively slowly.

Multi-phase flowmeters [9]

Currently, the application of *ECT* is being studied in the development of multiphase flowmeters. This is still in the research sector, and the study focuses on developing optimal techniques to measure various parameters for three-phase flows from the flow regimes, and modifying the current ECT design for achieving better resolution.

X. CONCLUSIONS

The *ECT* systems can be used for studying the chemical process inside a pipe and helps in viewing the contents which hitherto were not visible. Various information like, spatial distribution, volume ratio, and velocity of flow of the materials inside the chemical vessels can be computed by examining the permittivity distribution images. Though the advantages of *ECT* include low cost, non-intrusive technique for measurement, and fast response, the technique provides images of low resolution. The *LBPA* technique is used to reconstruct permittivity distribution images in real-time but suffers from poor spatial resolution. The spatial resolution can be enhanced by iterative methods, but this leads to lower image acquisition rate. Resolution can also be increased either by going for more number of electrodes or by using complex higher order protocols. But for industrial applications, the *LBPA* coupled with sufficient number of iterations suffices the requirement. The improved resolution enhances the clarity of the images and more information can be deduced from the images. This increases the accuracy of the calculated parameters, and results in better design and control of the process.

Electrical Capacitance Tomography technique for studying the chemical process is still in the research sector, and studies are going on for improving the design from various perspectives. The latest developments in this filed were discussed in a symposium held at Indian Institute of Technology, Kanpur [10]. The phenomena taking place inside stirred vessels and reactors are still an enigma. If *ECT* systems become implemental, they can play a very important role in 'seeing the chemical process without eyes'. An improved resolution of the images aids in judicious interpretation of the process. Hence, the scope for future work lies in development of faster and efficient algorithms which yields high resolution images at higher image acquisition rates. Currently, ECT techniques lack ability in measuring the flow velocities of liquids which are moving slowly, and multiphase flows. Hence, scope also lies in developing suitable techniques, to solve this problem and constructing a product which helps in characterizing slow moving liquids, and flowmeters to study the flow regimes of multiphase flows.

REFERENCES

[1] Andrew Hunt, John Pendleton, and Malcolm Byars, "Non-intrusive Measurement of Volume and Mass using Electrical Capacitance Tomography", Process Tomography Limited, Cheshire, United Kingdom.

[2] Malcolm Byars, "Developments in Electrical Capacitance Tomography", Process Tomography Limited, Cheshire, United Kingdom.

[3] Unpublished class notes of EE -617, Prof. L. R. Subramanyan, Department of Electrical Engineering, I ndian Institute of Technology, Bombay.

[4] Application Note AN 3, "Engineering Design Rules for ECT Sensors", Issue 4, March 2001, Process Tomography Limited, Cheshire, United Kingdom.

[5] Application Note AN 1, "Generation of ECT Images from Capacitance Measurements", Issue 3, March 2001, Process Tomography Limited, Cheshire, United Kingdom.

[6] Application Note AN 5, "Calculation of Normalized Capacitances", Issue 1, January 2000, Process Tomography Limited, Cheshire, United Kingdom.

[7] Application Note AN 4, "An Iterative Method for Improving ECT Images", Issue 2, April 1999, Process Tomography Limited, Cheshire, United Kingdom.

[8] Application Note AN 2, "Calculation of Volume Ratio for Sensors", Issue 4, October 1999, Process Tomography Limited, Cheshire, United Kingdom.

[9] Ahmed Abou-arkoub, Richard Thorn, and Amar Bousbain, "Modelling and Analysis of In -Situ validation Technique for Multiphase Flowmeters", IEEE Real -Time and Embedded Technology and Applications symposium.

[10] Prof. Prabhat Munshi, Department of Mechanical Engineering, Indian Institute of Technology, Kanpur, CT2004-Workshop on Computerized Tomography for Scientists and Engineers, Feb 13-15, 2004, Kanpur, India. http://home.iitk.ac.in/~pmunshi/ct2004_schedule.doc